# First Measurements of the Inclined Boron Layer Thermal-Neutron Detector for Reflectometry

T. L. van Vuure, J. F. Ankner, J. F. Browning, L. G. Clonts, M. L. Crow, R. G. Cooper, I. Remec, J. D. Richards, R. A. Riedel, and J. L. Robertson

***Abstract*—A prototype detector based on the inclined boron layer principle is introduced. For typical measurement conditions at the Liquids Reflectometer at the Spallation Neutron Source, its count rate capability is shown to be superior to that of the current detector by nearly two orders of magnitude.**

***Index Terms*—Boron, neutron detectors, position sensitive particle detectors, reflectometry.**

## I. Introduction

THE Spallation Neutron Source (SNS) in Oak Ridge, USA, is the first MegaWatt class pulsed neutron source. Building up a set of scattering instruments to match the facility presents many difficulties. Due to the high flux, most instruments will experience difficulties in dealing with the expected count rate. This is due, at least in part, to the available detectors.

For example, consider the Liquids Reflectometer [1], which is a general purpose neutron reflectometer for horizontal surfaces, including liquid-gas interfaces. It is mainly used for specular reflectometry, which characterizes structure normal to the surface, i.e., layers. Its main advantage over similar instruments at other facilities is the available high flux [2]. Because it has only recently been commissioned, it is still undergoing improvement. The intense reflected beam on the detector can cause a count rate of $> 10^6$ cps in a small area, typically 30 mm wide and 1–10 mm high. The detector needs to be able to deal with this massive data rate, have a time resolution of 10 $\mu$s and a spatial resolution of 1 mm vertically, as well as some more minor requirements. The current detector, a 2D position-sensitive Multi-Wire Proportional Counter (MWPC) from Brookhaven National Laboratory (BNL), fulfills all these requirements admirably, except for one. Because it has a global dead time of $\sim 2$ $\mu$s, at 10% dead time the instantaneous event rate is limited to 50 kcps globally. Using the standard 0.1–0.4 nm bandwidth at the Liquids Reflectometer, the instantaneous flux varies by an order of magnitude during each pulse. To operate at 10% dead time even during the high flux part of the pulse, the detector can only tolerate a time-averaged count rate of 3 kcps globally.

For this instrument and a few others, the Inclined Boron Layer Thermal-Neutron Detector (a technique proposed [3] at Institut Laue-Langevin, France) will alleviate some of the concerns because of its potential for high event rate operation.

Manuscript received March 02, 2009; revised September 20, 2009. Current version published February 10, 2010. This work was authored by UT-Battelle, LLC, under Contract DE-AC05-00OR22725 with the U.S. Department of Energy. The U.S. Government retains, and the publisher, by accepting the article for publication, acknowledges that the U.S. Government retains a non-exclusive, paid-up, irrevocable, world-wide license to publish or reproduce the published form of this manuscript, or allow others to do so, for U.S. Government purposes.

The authors are with the Spallation Neutron Source, Oak Ridge National Laboratory, Oak Ridge, TN 37830-8050 USA (e-mail: vanvuuretl@ornl.gov).

Color versions of one or more of the figures in this paper are available online at http://ieeexplore.ieee.org.

Digital Object Identifier 10.1109/TNS.2009.2036913

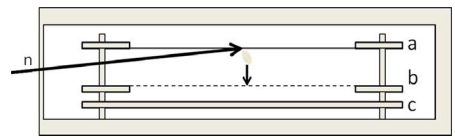


Fig. 1. Schematic representation of the inclined boron layer neutron detection principle.

## II. Principle of Detection of the Inclined Boron Layer

The Inclined Boron Layer Thermal-Neutron Detector is based on the well-known principle of exposing a suitable neutron absorber, boron, to the beam while suspended in a counting gas [4]. Upon absorption of a thermal neutron, $^{10}$B undergoes the following reaction (1):

$$^{10}\mathrm{B} +^{1} n \rightarrow^{7} \mathrm{Li}^{*} +^{4} \mathrm{He} + 2.3\,\mathrm{MeV}. \tag{1}$$

In 93% of all interactions, a $^{7}$Li$^{*}$ excited nucleus is produced, as indicated in (1), which decays shortly thereafter by gamma emission. In 7% of the cases, a $^{7}$Li in the ground state is produced, in which case the full 2.8 MeV neutron binding energy is available to the daughter products. In either case, these may exit the layer to deposit some of their energy in the gas, where a gaseous ionizing-radiation detector can be used to determine time and position of the interaction.

By inclining the absorber layer towards the incoming beam as indicated in Fig. 1, the grazing incident angle allows a larger proportion of neutrons to be absorbed in the first few microns of the layer, where the resulting secondary particles have a higher probability of escaping into the counting gas. This leads to an increase in efficiency that is angularly dependent [5]. As a side effect, this also leads to a spreading out of events over a wider area, allowing the detector to deal with higher count rates. Additionally, it leads to a higher effective spatial resolution in one direction. This happens to be desirable for reflectometry.

Fig. 1 illustrates the detection principle. Neutrons, indicated with "n", enter from the left. Upon absorption in the $^{10}$B layer ("a") which is exposed to the gas, secondary particles liberate a cloud of electrons in the counting gas, which drifts under the

0018-9499/$26.00 © 2010 IEEE

Authorized licensed use limited to: Oak Ridge National Laboratory. Downloaded on February 11, 2010 at 09:35 from IEEE Xplore. Restrictions apply.

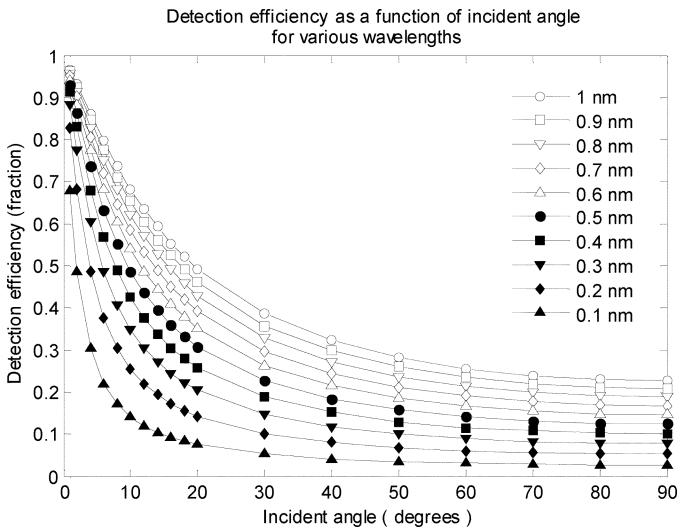


Fig. 2. Simulation results for detection efficiency given a 2 $\mu$m thick $^{10}$B absorber layer as a function of incident angle, given for neutron wavelengths from 0.1 nm (82 meV) up to 1 nm (0.82 meV).

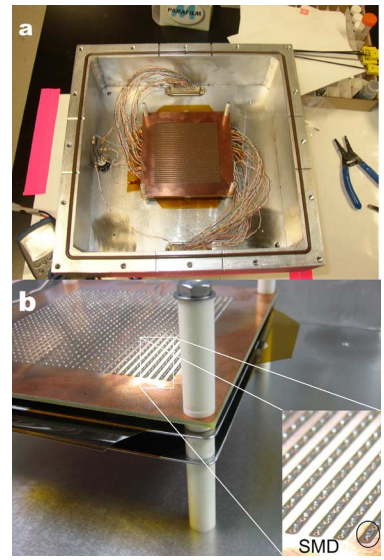


Fig. 3. Photos of the interior of the prototype detector. The inset shows the Surface Mountable Device (SMD) resistors that interconnect the anode pixels, which are themselves not visible because they are located on the opposite side of the frame.

influence of an electric field towards the Gas Electron Multiplier (GEM), indicated with "b", in the direction indicated by the small arrow. The induced current is observed on the pad read-out ("c") after multiplication by the GEM.

## III. Monte Carlo Model

A Monte Carlo model was written to simulate the neutron interactions in the detector. By writing the code from the ground up, a deeper insight in the workings of the detection principle was gained. In order to test the validity of the code, its results were compared against those of PHITS (Particle and Heavy Ion Transport code System [6]). The following steps were modeled:

- arrival of the neutron at the absorber layer with a predefined angle and wavelength
- absorption in the layer in a random location along the flight path, with positions sampled from a probability distribution following from the appropriate reaction cross sections
- back-to-back emission of the reaction products in a random direction, with an isotropic distribution
- tracking of the energy loss of the particles in the solid absorber layer, assuming uniform energy loss along the track to simplify the calculation
- tracking of the energy loss in the gas volume, also assuming uniform energy loss
- determining the centroid of the deposited energy in the gas, along with its total magnitude

By tabulating the number of events that deposit more energy in the gas than a certain threshold value, usually set to 200 keV, the resulting data could be used to determine detection efficiency as a function of incident angle or neutron wavelength, see Fig. 2.

Assuming a standard pixel or strip read-out, the resulting spatial resolution could be estimated as well from the distribution of the Center-Of-Gravity (COG) of the tracks in the gas.

## IV. Prototype

A prototype has been constructed to test the inclined layer detection principle, and is shown in Fig. 3(a).

As a counting gas, Ar/$CO_2$ 90/10 was used at 0.8 bar absolute pressure (80 kPa). The prototype has been designed to hold an over- or underpressure of 1 bar maximum. Previous experience suggests that the GEM should be capable of an effective gas avalanche multiplication factor of $10^2$-$10^3$ without serious risk of catastrophic breakdown.

A suitable 2 $\mu$m thick deposit was made by CASCADE Detector Technologies GmbH (CDT, Hans-Bunte-Strasse 8–10 Heidelberg 69123, Germany) at a size of 10 cm by 10 cm. A Gas Electron Multiplier (GEM) [7] of the same size was used, followed by the detector anode in the form of a grid of pixels. These are mounted as shown in Fig. 3(b) on insulated poles with insulating spacers in between. Independent readout of each pixel was considered essential to be able to operate in the anticipated high flux. Since this would necessitate a considerable investment in individual readout channels, an intermediate solution was adopted where all pixels in each column are interconnected using resistors. The position within each column could then be calculated by charge division. Fig. 3(a) and (b) show these arrays, with an inset to show some of the individual resistors.

The experimental assembly is very similar to that in Fig. 1. The boron-coated drift cathode is located 10 mm away from the GEM. This volume is called drift gap. The induction gap is on the other side of the GEM and is 3 mm wide. The drifting charge, amplified in the GEM holes, induces signals on the neighboring anode pads.

In order to allow for easy integration of the detector in the existing infrastructure, the electronics and data acquisition developed at SNS [8] was used. A full description of this system is in preparation for publication. Pre-amplification was performed on a custom-designed and produced preamp

Authorized licensed use limited to: Oak Ridge National Laboratory. Downloaded on February 11, 2010 at 09:35 from IEEE Xplore. Restrictions apply.

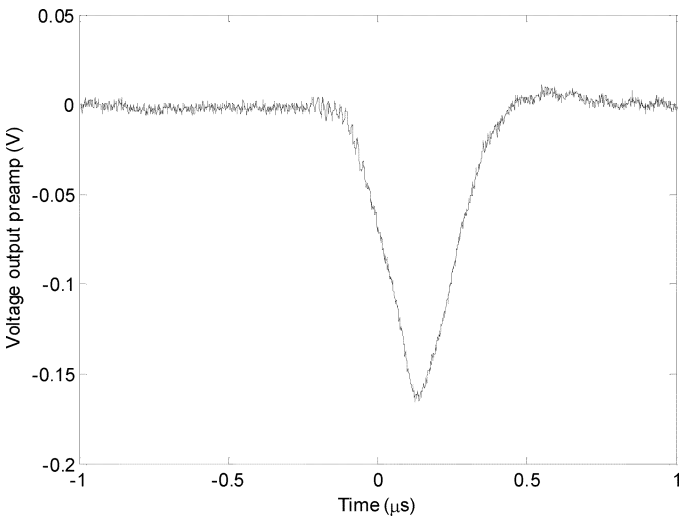


Fig. 4. Example of a neutron pulse, recorded with the prototype. A transimpedance amplifier was used with 200 ns rise time and 400 ns fall time.

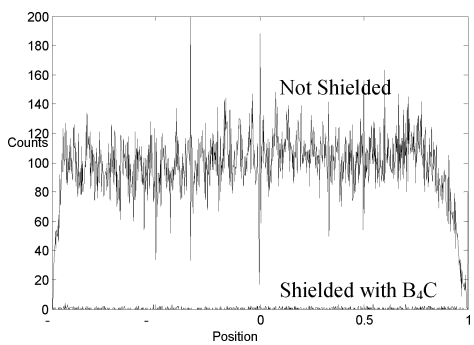


Fig. 5. Uniform irradiation of the prototype detector. Raw data is shown; artifacts smaller than the spatial resolution of the detector have not been removed. The top curve shows neutrons from a moderated $^{252}\mathrm{Cf}$ source, the bottom shows the same source shielded with $\mathrm{B_4C}$.

board, which used a trans-impedance amplifier with a rise- and fall time of $\sim 200$ ns. This signal was then exported with Low-Voltage Differential Signaling (LVDS) using a commonly available category 5e cable. A Read-Out Card (ROC board) triggered on a signal when crossing a threshold. Subsequently, a fixed-time integrator was started, the output of which was sampled by an ADC. The ROC-board could perform charge division locally. Up to 8 ROC-boards could be connected to a Front End Module (FEM), and up to 5 FEMs could report to one Digital Signal Processor. All of these were optimized to handle the huge data rates encountered at the SNS.

## V. First Measurements

The first measurements with this prototype have been performed at the SNS detector test port at the High Flux Isotope Reactor (HFIR) in Oak Ridge. Fig. 4 shows an example of a neutron pulse.

Fig. 5 shows data from a uniform irradiation of the detector, with the neutrons incident on the boron absorber surface in a roughly perpendicular orientation. This was performed using a moderated $^{252}\mathrm{Cf}$ test source. The simple expedient of inserting a sheet of $\mathrm{B_4C}$ sufficed to show that the overwhelming majority of these events were due to thermal neutrons.

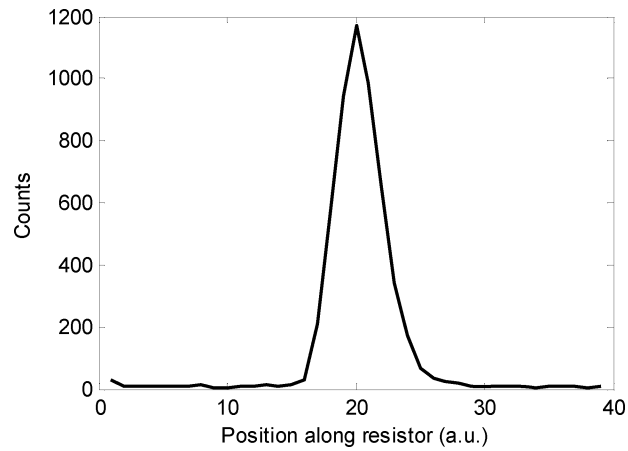


Fig. 6. Foot print of a 1 mm wide neutron beam in the detector, inclined at a grazing incident angle of 6°.

Three types of artifacts are visible in Fig. 5:

- Sharp spikes, a single bin wide, caused by digitized division logic errors.
- A 33 fold saw tooth pattern caused by the 33 pixels in each column, which are interconnected by resistors. A continuous resistor, such as a resistive anode in a tube, does not exhibit this behavior.
- A slow variation in count rate across the surface, presumably due to non-uniformity across the detector in both the local GEM gain and the boron layer thickness.

Only the third artifact type is relevant to the operation of the detector. The other two show irregularities of 1 pixel or less, which means smaller than the resolution limit of the detector. In later results below, larger bins are used to report the measured position, which removes the artifacts. However, it is still useful to show this behavior since it increases the understanding of the detector.

Fig. 6 shows a visualization of the beam footprint using the 0.425 nm (4.5 meV) neutrons from the SNS detector test port at HFIR. The beam was collimated to $\sim 1$ mm wide when it reached the detector, which was positioned at a suitable angle.

The Full Width at Half Maximum (FWHM) of the beam as recorded by the detector was about 10 mm, which at an inclination of 6° represented a height of 1 mm. This was also the height of the beam at the detector position. Since the recorded beam height was a convolution of the real beam height with the detector resolution, we can conclude that the detector resolution did not contribute an appreciable amount to the recorded beam height. It must therefore have a value better than 1 mm, but estimating it is impossible based on these data and further measurements with better collimation will be required.

Because the plastic substrate of the $^{10}\mathrm{B}$ is not perfectly flat, the incoming neutron beam can hit "valleys" or "hills" depending on the exact local geometry. This causes a dependence of the recorded size of the beam footprint on the position. Because the angle of incidence also varies with local geometry, there is a modulation of the detection efficiency at small incident angles, see Fig. 7. Note also that local efficiency

Authorized licensed use limited to: Oak Ridge National Laboratory. Downloaded on February 11, 2010 at 09:35 from IEEE Xplore. Restrictions apply.

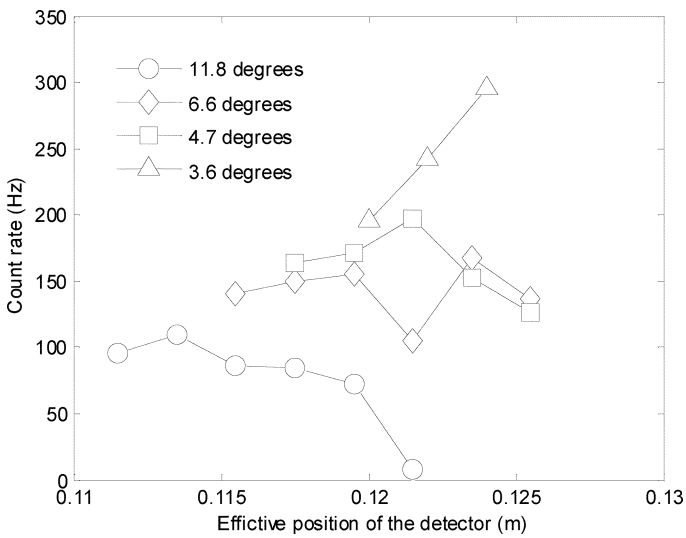


Fig. 7. Response (in terms of count rate) of the detector as a function of position. Large non-uniformities are visible, presumably due to surface modulations (non-flatness). Small wrinkles in the plastic substrate for the $^{10}$B layer can locally result in an effective angle of incidence of the beam that is a few degrees off the average value.

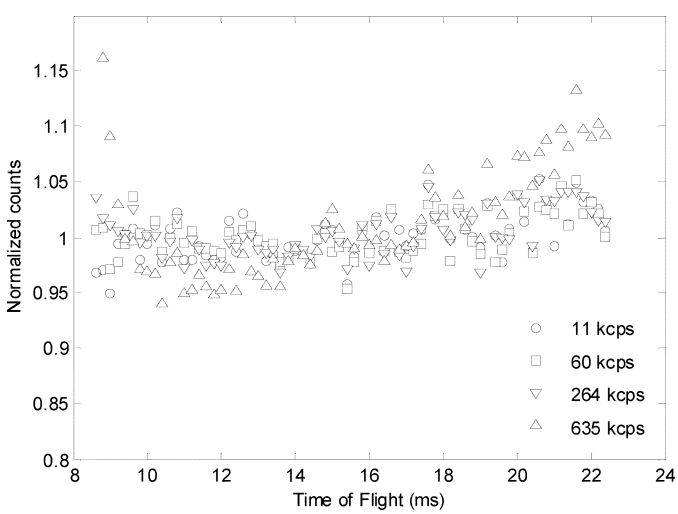


Fig. 8. Time of Flight spectra at various count rates, normalized to the spectrum at 1.5 kcps, which is considered not to be deformed by pile-up effects.

variations of up to 50% are found. This illustrates the need for a flat and rigid substrate for the $^{10}$B layer. At higher angles, another limitation becomes evident; at certain positions, the frame holding the GEM can move into the beam, disturbing the beam and essentially cutting it to zero.

In order to experimentally determine the count rate capability of the detector, it was placed in the beam at the Liquids Reflectometer at SNS.

The maximum recorded time-averaged count rate in these experiments was 635 kcps. However, routine operations at the Liquids Reflectometer require the dead time to be kept well below 10%, to limit pile-up effects that can distort the recorded Time of Flight (ToF) spectra. An example of this distortion can be seen in Fig. 8 for the measurement recorded with the highest event rate. Because these spectra are normalized to a single spectrum at low rate, distortion shows up as a deviation from unity. The

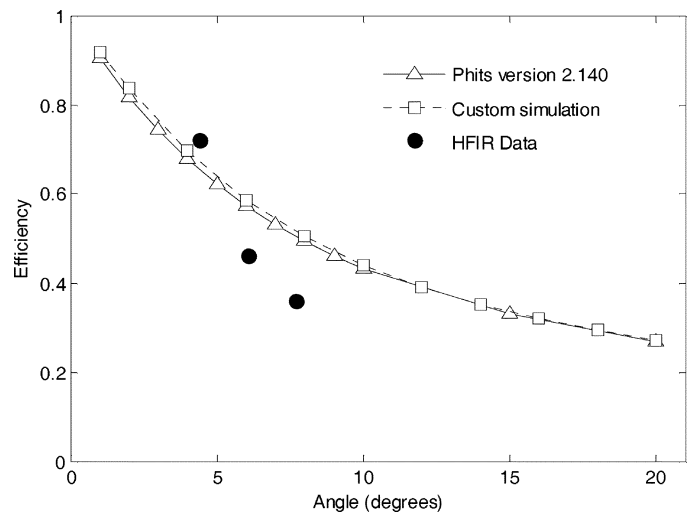


Fig. 9. Detection efficiency as a function of incident angle for several neutron wavelengths. Absorber layer was 2 $\mu$m $^{10}$B. Data points were taken at 0.425 nm (4.5 meV).

highest time-averaged count rate at which the detector has been demonstrated to meet this criterion was 264 kcps. This represents an improvement of nearly two orders of magnitude over the detector that is currently in use at the reflectometer.

By recording the count rate as a function of the incident angle, the predictions of the Monte Carlo simulations could be tested (see Fig. 9). For these measurements a relatively wide beam was used at HFIR in order to average out non-uniformities. The correspondence between measurement and simulation is only qualitative, the angular dependence seems much sharper than simulations suggest. No satisfactory explanation for this discrepancy has been found. On the other hand, the agreement between the Monte Carlo code PHITS and the custom code is reasonable, to within 5%. It should be noted that at an incident angle comparable to the divergence, $\sim 0.1^\circ$ in this case, the efficiency will be harder to calculate. Additionally, below that angle surface reflectivity becomes an issue.

## VI. Conclusions

A prototype detector, based on the principle of the inclined boron layer, was tested at the Spallation Neutron Source. A solid layer of thermal-neutron absorber was suspended in a neutron-transparent counting gas under a grazing incident angle to a neutron beam, and events which deposited energy in the counting gas over a certain threshold were recorded using a Gas Electron Multiplier.

Monte Carlo simulations showed that the efficiency was expected to be a function of angle of incidence on the detector, as well as of neutron wavelength. Experiments did show this dependence, but were not in quantitative agreement with the simulations.

Because the Liquids Reflectometer at the SNS is currently limited by the count rate capability of its detector, a MWPC, the detector was tested under high flux. It has been shown to handle a time-averaged event rate of 264 kcps. At that event rate, the dead time is kept low enough to avoid visible distortion of the ToF spectra, even during the highest-flux period of each neutron

Authorized licensed use limited to: Oak Ridge National Laboratory. Downloaded on February 11, 2010 at 09:35 from IEEE Xplore. Restrictions apply.

pulse. This represents an improvement of nearly two orders of magnitude over the current detector.

## REFERENCES

[1] J. F. Ankner, X. Tao, C. E. Halbert, J. F. Browning, S. M. Kilbey, II, O. A. Swader, M. S. Dadmun, E. Kharlampieva, and S. A. Sukhishvili, "The SNS liquids reflectometer," *Neutron News*, vol. 19, no. 3, pp. 14–16, 2008.

[2] J. F. Ankner, M. Jansma, E. D. Blakeman, and R. L. Kellogg, "The optical design of the SNS liquids reflectometer," *Appl. Phys. (Suppl.)*, vol. A74, pp. 1610–1612, 2002.

[3] B. Guérard *et al.*, "Advances in detectors for single crystal neutron diffraction," *Nucl. Instrum. Methods Phys. Res. A*, vol. A554, pp. 392–405, 2005.

[4] H. Friedrich, V. Dangendorf, and A. Bräuning-Demian, "Position-sensitive thermal neutron detector with $^{6}$Li-foil converter coupled to wire chambers," *Appl. Phys. A*, vol. 74, pp. 124–126, 2002.

[5] T. L. van Vuure, Proposal for the Design and Construction of an Inclined Boron Layer Thermal-Neutron Detector for the Reflectometer at SNS, internal ORNL publication, 21617.

[6] H. Iwase, K. Niita, and T. Nakamura, "Development of general-purpose particle and heavy ion transport Monte Carlo code," *J. Nucl. Sci. Technol.*, vol. 39, pp. 1142–1151, 2002.

[7] F. Sauli, "GEM: A new concept for electron amplification in gas detectors," *Nucl. Instrum. Methods Phys. Res. A*, vol. A386, p. 531, 1997.

[8] R. A. Riedel and R. G. Cooper, "The 8-pack read-out electronics chain at the Spallation Neutron Source," Tech. Notes, ORNL.

Authorized licensed use limited to: Oak Ridge National Laboratory. Downloaded on February 11, 2010 at 09:35 from IEEE Xplore. Restrictions apply.